

# Theta functions and optimal lattices for a grid cells model

Laurent Bétermin

Faculty of Mathematics, University of Vienna,  
Oskar-Morgenstern-Platz 1, 1090 Vienna, Austria  
`laurent.betermin@univie.ac.at`. ORCID id: 0000-0003-4070-3344

June 10, 2022

## Abstract

Certain types of neurons, called “grid cells” have been shown to fire exactly on a triangular grid when an animal is navigating on a two-dimensional environment, whereas recent studies suggest that the face-centred-cubic (FCC) lattice is the good candidate in three dimensions. The goal of this paper is to give new evidences of these phenomena by considering a infinite set of independent neurons (a module) with Poisson statistics and periodic long-range Gaussian tuning curves. This question of the existence of an optimal grid is transformed into a maximization problem among all possible unit density lattices for a Fisher Information which measures the accuracy of grid-cells representations in  $\mathbb{R}^d$ . This Fisher Information has translated lattice theta functions as building blocks. We first derive asymptotic and numerical results showing the (non-)maximality of the triangular lattice with respect to the Gaussian parameter and the size of the firing field. In the case of radially symmetric distribution of firing locations, we also characterize all the lattices that are critical points for the Fisher Information at fixed scales which belong to an open interval (also called “volume stationary”). It allows us to compare the Fisher Information of a finite number of lattices in dimensions 2 and 3 and to give another evidences of the optimality of the triangular and FCC lattices.

**AMS Classification:** Primary 49N20; Secondary 62P10.

**Keywords:** Grid cells, Lattices, Optimization, Fisher Information, Theta functions.

## Contents

<b>1</b>	<b>Introduction and setting</b>	<b>2</b>
1.1	Presentation of the problem . . . . .	2
1.2	Some known results on optimal lattices . . . . .	4
1.3	Numerical and asymptotic results . . . . .	5
1.4	Characterization of volume-stationary lattices . . . . .	6
1.5	Conclusion and open problems . . . . .	7
<b>2</b>	<b>Description of the model, derivation of formula (1.3) and scaling</b>	<b>7</b>
<b>3</b>	<b>Alternative formula and proof of Theorem 1.2</b>	<b>10</b>
<b>4</b>	<b>Volume-stationary lattices - Proof of Theorem 1.4</b>	<b>11</b>
<b>5</b>	<b>Numerical investigation</b>	<b>12</b>
5.1	Parametrization of lattices in dimension 2 and 3 . . . . .	12
5.2	The pure discrete case: combinations of $\mathcal{Q}_L(y)$ . . . . .	12
5.3	Dimension 2 . . . . .	14
5.4	Dimension 3 . . . . .	16

# 1 Introduction and setting

## 1.1 Presentation of the problem

A challenging mathematical problem is to justify rigorously why periodic patterns arise in nature and experiments: densest packing [17, 46], atoms in a solid [26, 34], triangular lattices of Ginzburg-Landau vortices in type II superconductors [1, 38], rich polymorphic behavior for systems with Coulombian interactions [3, 29], etc. This type of problem, also called “Crystallization problem” (see [15]), is often considered as variational, which means that optimal periodic structures can be seen as extrema of certain functionals usually derived from simplified models.

An typical example in Neurobiology is the existence of grid cells in the medial entorhinal cortex (MEC) of the brain discovered by Hafting et al. [24] and that have been found in many mammals (rats, humans, etc.) as recalled in [37]. Each of these neurons is tuned to the position of the animal and fires when it crosses the sites of an approximate triangular lattice (also called “hexagonal lattice”, see (1.7) for a precise formula and Fig. 2 for a representation) during two-dimensional navigation. Furthermore, several evidences have been found in the brains of flying bats and humans for face-centred-cubic (FCC) lattices encoding the spatial representation in three-dimensional displacements (see e.g. [27, 48]). Grid cells can be split into modules where the firing periodic patterns share the same scale and orientation but are shifted around an average position belonging to a firing field (i.e. the connected spatial region that evokes firing). Also, the scales of the grids vary in a discrete way throughout the MEC as shown in [42]. Therefore, explaining why one module is tuned to a triangular or FCC lattice pattern is a crucial question.

Several Mathematical attempts to justify the emergence of the triangular grid for one module have been made (see e.g. [2, 19, 31, 36, 40, 41, 45, 47]), and the present work is inspired by the one of Mathis et al. [31] where an Information Theory point of view has been chosen. The goal is to maximize the Fisher Information’s trace measuring the accuracy of grid cells representations. The main novelties in our work with respect to [31] is that we are not using asymptotic arguments to simplify the model which allows Mathis et al. to treat the optimality question as a best packing problem leading to the triangular and FCC lattices as optimizers. Furthermore, we are considering long-range Gaussian tuning curves instead of short-range bump functions. All these new assumptions transform the short-range packing problem [31] into a long-range energy maximization problem as the hard-sphere crystallization question [25] was transformed into a minimization question among lattices for Gaussian interactions in [32].

We now briefly introduce our setting. The reader can refer to Section 2 for a complete derivation of our main formula based on several biologically relevant assumptions that are only partially recalled in this introduction for a complete understanding of the problem. The main statistical notions are also well explained in [28]. We assume that the neurons (grid cells) are independently firing and follow Poisson statistics. The average firing number of a neuron is given by a lattice periodic tuning curve  $\Omega_L^\alpha$  which tunes the position  $x \in \mathbb{R}^d$  of the animal to the positive real number  $\Omega_L^\alpha(x) \in \mathbb{R}_+$ , where

$$\Omega_L^\alpha(x) = \theta_{L+x}(\alpha) := \sum_{p \in L} e^{-\pi\alpha|p+x|^2}, \quad \alpha > 0, \quad L = \bigoplus_{i=1}^d \mathbb{Z}u_i, \quad (1.1)$$

the Euclidean norm being denoted by  $|\cdot|$  and  $\{u_i\}_{1 \leq i \leq d}$  is a basis of  $\mathbb{R}^d$ . Such  $L \subset \mathbb{R}^d$  is called a  $d$ -dimensional lattice and  $\theta_{L+x}(\alpha)$  is called the translated lattice theta function (see also [13]). Notice that the constant  $\pi$  is only here for technical reasons and to fit perfectly with the usual definition of theta function. We call  $\mathcal{L}_d(V)$  the set of lattices with co-volume  $V$ , i.e.

$$\mathcal{L}_d(V) = \left\{ L = \bigoplus_{i=1}^d \mathbb{Z}u_i : \{u_i\}_i \text{ basis of } \mathbb{R}^d, |\det(u_1, \dots, u_d)| = V \right\}.$$

Notice that the choice of a tuning curve of Gaussian type is biologically relevant (see e.g. [19, 22]) but our main formula will be written in Section 2 in terms of a general function  $f$ . However, since the translated theta function is traditionally seen as a building blocks for a large class of lattice energies, we have chosen to focus on this important case in this paper.

Since a module is given by a set of translated versions of the lattice  $\{L + y_j\}_j$  and tuning curves  $\Omega_{L+y_j}^\alpha(x)$ , we are assuming that the empirical measure  $\delta_Y$  associated with set of shifts  $Y = \{y_j\}_j$  converges to a Radon measure  $\mu$  (i.e. the firing distribution) with support  $\Sigma$  and called the firing field. We will write  $\mu \in \mathcal{M}(\Sigma)$ . It is well-known that  $\Sigma$  scales as the lattices (see e.g. [16]), in the sense that multiplying the lattice distances by  $\lambda > 0$  implies that we have to replace the firing field by  $\lambda\Sigma$ . In order to take the change of scaling into consideration, we define, for any  $\lambda > 0$ , the rescaled measure  $\mu_\lambda$  on the Borelian set  $\mathcal{B}_d$  of  $\mathbb{R}^d$  by

$$\mu_\lambda(F) = \mu(\lambda F), \quad \forall F \in \mathcal{B}_d. \quad (1.2)$$

Fig. 1 depicts the situation in  $\mathbb{R}^2$ . Our goal is to decode the position (e.g.  $x = 0$ ) of the animal given the number of spikes of a neuron population. Therefore, as in [31], we are considering the Fisher information  $J_M(0)$  per neuron associated to the module  $M := (L, \Omega_L^\alpha, \mu, \Sigma)$  whose the inverse of the trace is a lower bound for the error made in the decoding process. In our setting, the trace of  $J_M(0)$  is shown (see Section 2) to be

$$\mathcal{F}_\mu^\alpha(L) = \int_\Sigma \mathcal{Q}_L^\alpha(y) d\mu(y) \quad \text{where} \quad \mathcal{Q}_L^\alpha(y) := \left| \nabla_y \sqrt{\theta_{L+y}(\alpha)} \right|^2, \quad (1.3)$$

and the question we are investigating is to find the lattice for which the decoding error is the smallest possible, which is at the same time both biologically and mathematically interesting. The inverse of the Fisher Information's trace is known to be, via the Cramer-Rao bound, the lower bound of this error, that is why we want to maximize it.

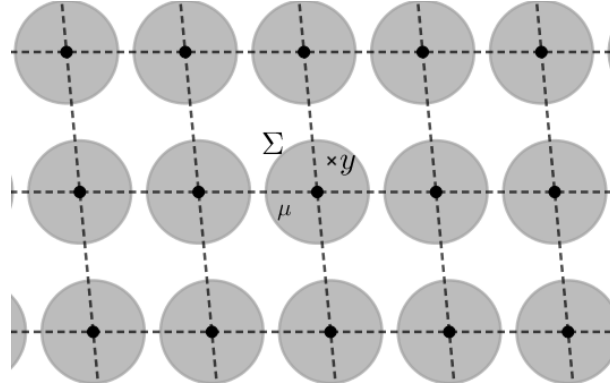


Figure 1: General configuration with lattice  $L$ , firing field  $\Sigma = B_R$  (repeated periodically) and a generic point  $y \in \Sigma$ .

According to the following scaling formula (see Proposition 2.2) true for any  $\alpha > 0$ ,  $\lambda > 0$ ,  $\Sigma \subset \mathbb{R}^d$ ,  $\mu \in \mathcal{M}(\Sigma)$  and  $L \in \mathcal{L}_d(1)$ ,

$$\mathcal{F}_{\mu_\lambda}^\alpha(\lambda L) = \lambda^{-2} \mathcal{F}_\mu^{\lambda^2 \alpha}(L), \quad (1.4)$$

it is then enough to consider unit density lattices in our problem stated as follows.

**Maximization Problem:** Given  $\alpha > 0$  and  $\mu$ , what is the maximizer of  $\mathcal{F}_\mu^\alpha$  in  $\mathcal{L}_d(1)$ ?

**Remark 1.1.** It is implicit that  $\Sigma$ , i.e. the support of  $\mu$ , is also fixed in the above problem. Furthermore, it has been observed that firing fields do not overlap and our numerics will show in Section 5 the fact that too much overlapping implies the non-existence of a maximizer for  $\mathcal{F}_\mu^\alpha$  in  $\mathcal{L}_2(1)$ , therefore confirming this fact.

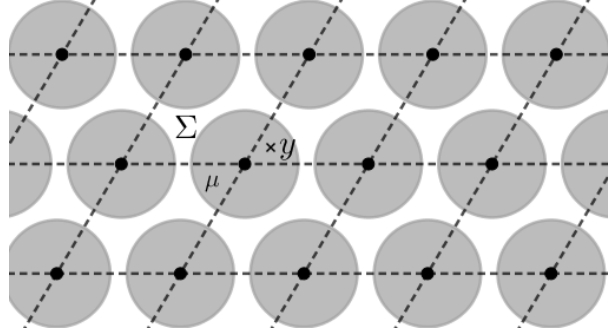


Figure 2: Triangular configuration with lattice  $A_2$  defined by (1.7), firing field  $\Sigma = B_R$  (repeated periodically) and a generic point  $y \in \Sigma$ .

In this paper, we are giving several types of results concerning this maximization problem: asymptotic, numerical and constrained. Indeed, it appears that finding a rigorous proof of any optimality result for  $\mathcal{F}_\mu^\alpha$ , where  $\alpha, \mu$  are fixed, is out of reach. However, it is possible to study the behaviour of the functional as  $\alpha \rightarrow 0$  or numerically when the parameters are fixed. Furthermore, staying in the class of lattices that are critical points of  $\mathcal{F}_\mu^\alpha$  in an open interval of scales, which is biologically relevant, leads to comparing only a finite number of highly symmetric lattices.

## 1.2 Some known results on optimal lattices

The type of optimality problem investigated in this paper has attracted recently a lot of attention (see e.g. [15, Sect. 2.5]), especially in Mathematical Physics for energies per point of type

$$E_f[L] := \sum_{p \in L} f(|p|^2), \quad \text{where} \quad |f(r)| = O(r^{-\frac{d}{2}-\eta}), \eta > 0 \quad \text{as } r \rightarrow +\infty, \quad (1.5)$$

and where  $f$  is interpreted as an interaction potential between particles. The exponential case – i.e. where  $f(r^2) = e^{-\pi\alpha r^2}$ ,  $\alpha > 0$ , is a Gaussian function – appears to be of fundamental importance. In this case, the energy defined in (1.5) is called the lattice theta function

$$\theta_L(\alpha) := \sum_{p \in L} e^{-\pi\alpha|p|^2}, \quad (1.6)$$

which appears to be a building block for any energy of type  $E_f$  where  $f = \mathcal{L}(\mu_f)$  is the Laplace transform of a measure  $\mu_f$  on  $\mathbb{R}_+$  (see e.g. [14]). When  $\mu_f$  is positive, then  $f$  is called completely monotone and the optimality of a lattice in  $\mathcal{L}_d(1)$  for  $L \mapsto \theta_L(\alpha)$  and for any given  $\alpha > 0$  ensures the same result for  $E_f$ . If we allow our structures  $L$  to be more general periodic configurations, then such optimality result is called universal optimality and has been solved in dimensions  $d \in \{8, 24\}$  in [18] where the best packings (see [17, 46])  $E_8$  and  $\Lambda_{24}$  are the unique minimizers in the respective dimensions. However, this problem is still open in dimension  $d = 2$  where the triangular lattice

$$A_2 := \sqrt{\frac{2}{\sqrt{3}}} \left[ \mathbb{Z}(1, 0) \oplus \mathbb{Z} \left( \frac{1}{2}, \frac{\sqrt{3}}{2} \right) \right], \quad (1.7)$$

which is the two-dimensional best packing, is conjectured to be the unique minimizer. When restricted to the set of lattices, the lattice theta function has been shown by Montgomery [32] to be minimized by  $A_2$  for any  $\alpha > 0$ . Furthermore, such result cannot be true in dimension  $d = 3$  as explained in [39] since the best candidates, which are the Face-Centred-Cubic (FCC) and Body-Centred-Cubic (BCC) lattices respectively defined by

$$D_3 := 2^{-\frac{1}{3}} [\mathbb{Z}(1, 0, 1) \oplus \mathbb{Z}(0, 1, 1) \oplus \mathbb{Z}(1, 1, 0)]$$

$$\mathbf{D}_3^* := 2^{\frac{1}{3}} \left[ \mathbb{Z}(1, 0, 0) \oplus \mathbb{Z}(0, 1, 0) \oplus \mathbb{Z}\left(\frac{1}{2}, \frac{1}{2}, \frac{1}{2}\right) \right]$$

are dual of each other but not unimodular, i.e.  $\mathbf{D}_3^* \neq \mathbf{D}_3$ . We recall that the dual lattice of  $L$  is defined by  $L^* = \{y \in \mathbb{R}^d : y \cdot p \in \mathbb{Z}, \forall p \in L\}$ .

The extrema of the translated theta function  $(L, y) \mapsto \theta_{L+y}(\alpha)$  have also been studied. On the one hand, all the critical points of  $y \mapsto \theta_{L+y}(\alpha)$  as well as their nature are known when  $L$  is an orthorhombic (see [13, Sect. III.3]) or triangular lattice (see [5]) and for all  $\alpha > 0$  and only the trivial one are known in general (center of the cell and midpoints). Therefore, all the zeros of  $\mathcal{Q}_L^\alpha$  are also known in these cases. On the other hand, only few results are available concerning the extrema of  $L \mapsto \theta_{L+y}(\alpha)$  for fixed  $y \neq 0$ , namely the case where  $y = c_L$  is the center of the unit cell of  $L$ . In that case,  $L \mapsto \theta_{L+c_L}(\alpha)$  does not have any minimizer (see [13, Prop. 1.3]) and the maximizer among two-dimensional lattices (resp. among  $d$ -dimensional orthorhombic lattices) with the same density is the triangular lattice  $\mathbf{A}_2$  (resp. the simple cubic lattice  $\mathbb{Z}^d$ ) as we have shown in [10] (resp. in [13, Thm. 1.4] by mainly using tools from [21]). Notice that other two-dimensional results of this type might be derived from new discoveries concerning combinations of theta functions [30].

Concerning the averaging of the shifts for the lattice theta functions, i.e. for energies of the form  $\int_\Sigma \theta_{L+y}(\alpha) d\mu(y)$ , recent advances have been made in [9, 12] when  $\mu$  is radially symmetric, sufficiently rescaled around the origin, or generated by a completely monotone kernel  $\rho$  as  $d\mu(x) = \rho(|x|^2)dx$ . In particular, the above mentioned results for the lattice theta function  $L \mapsto \theta_L(\alpha)$  on  $\mathcal{L}_d(1)$  still hold in these cases for  $L \mapsto \int_\Sigma \theta_{L+y}(\alpha) d\mu(y)$ .

### 1.3 Numerical and asymptotic results

Whereas  $\mathcal{F}_\mu^\alpha$  defined by (1.3) has the translated lattice theta function  $\theta_{L+y}(\alpha)$  as a building block (or the Heat Kernel on  $L$ , see Remark 2.1), it cannot be considered like a lattice energy of type  $E_f$  defined by (1.5). It is also clear that finding the global maximizer of  $\mathcal{F}_\mu^\alpha$  using an analytic or variational method is out of reach but numerically accessible. Moreover, some asymptotic results can be shown.

It is indeed usual to study the asymptotic behaviour with respect to  $\alpha$  of a problem involving lattice theta functions (see e.g. [13, Thm. 1.6]). When  $\alpha \rightarrow 0$ , an alternative formula (see (3.1)) using a recent result by Regev and Stephens-Davidowitz in [35] combined with new results on the soft lattice theta function lead to the following asymptotic result.

**Theorem 1.2 (The small  $\alpha$  case).** *Let  $\mu \in \mathcal{M}(\Sigma)$  be radially symmetric and  $\Sigma = B_R \subset \mathbb{R}^2$ , for some  $R > 0$ , its support. Then:*

1. *For all  $L \in \mathcal{L}_2(1)$ ,  $\exists \alpha_0 > 0$ ,  $\exists \lambda_0 > 0$ , such that for all  $\alpha < \alpha_0$ , for all  $\lambda < \lambda_0$ ,*

$$\mathcal{F}_{\mu_\lambda}^\alpha(L) > \mathcal{F}_{\mu_\lambda}^\alpha(\mathbf{A}_2).$$

2. *For  $\mu$  such that  $d\mu(x) = \rho(|x|^2)dx$ , where  $\rho$  is a completely monotone function and all  $L \in \mathcal{L}_2(1)$  there exists  $\alpha < \alpha_0$  such that  $\mathcal{F}_\mu^\alpha(L) > \mathcal{F}_\mu^\alpha(\mathbf{A}_2)$ .*
3. *There exists  $\alpha_1 > 0$  and  $\lambda_1 > 0$  such that for all  $0 < \alpha < \alpha_1$  and  $0 < \lambda < \lambda_1$ ,  $\mathcal{F}_{\mu_\lambda}^\alpha$  does not have any maximizer in  $\mathcal{L}_2(1)$ .*

*In dimensions  $d = 3$ , the two first points are true for  $L$  in an open ball of  $\mathcal{L}_3(1)$  centred at  $\mathbf{D}_3^*$  and the third point also holds.*

This result agrees with the numerics we have performed for small  $\alpha$  and where the triangular lattice minimizes  $\mathcal{F}_\mu^\alpha$  (see Fig. 9). Furthermore, our main numerical findings are the following (see Section 5), choosing  $\Sigma = B_R$ ,  $\mu = \sigma_R$  being the uniform measure on  $B_R$  and  $\alpha = \frac{10}{\pi}$ :

- **Dimension 2. Maximality of the triangular lattice.**

- **Global optimality of the triangular lattice.** The triangular lattice  $A_2$  is the unique maximizer of  $\mathcal{F}_\mu^\alpha$  in  $\mathcal{L}_2(1)$  for  $R \in \left\{0.1, 0.2, 0.3, 0.4, 0.5, \frac{1}{2}\sqrt{\frac{2}{\sqrt{3}}}\right\}$ . The last value of  $R$  corresponds to half of the side length of  $A_2$ .
- **Non-existence of a maximizer for large  $R$ .** If  $R \geq 0.59$ , then  $\mathcal{F}_\mu^\alpha$  does not have a maximizer in  $\mathcal{L}_2(1)$  and  $A_2$  is its unique minimizer in  $\mathcal{L}_2(1)$ .

- **Dimension 3. Maximality of the FCC lattice**

- **Comparison of cubic lattices.** There exists  $R_0 \approx 0.57$  such that for all  $R \leq R_0$ ,

$$\mathcal{F}_\mu^\alpha(D_3) > \mathcal{F}_\mu^\alpha(D_3^*) > \mathcal{F}_\mu^\alpha(\mathbb{Z}^3).$$

- **Local maximality of the FCC lattice.**  $D_3$  is a local maximizer of  $\mathcal{F}_\mu^\alpha$  in  $\mathcal{L}_3(1)$  for  $R \in \{0.1, 0.2, 0.3, 0.4, 0.5, 2^{-5/6}\}$ . The last value of  $R$  corresponds to half of the side length of  $D_3$ .

According to the scaling formula (1.4), the same qualitative behaviour holds for any other value of  $\alpha$  with rescaled quantities.

#### 1.4 Characterization of volume-stationary lattices

In [42], it has been observed that rats have grid cells with grid spacing from 35.2cm to 171.7cm, from dorsal to ventral MEC. The set of possible scales has been shown to be discrete for all the studied species, with different values. If we believe that grid cell is something universal among a lot of species, in such a way that grid scales are covering all the possible values of a certain (open) interval, we can focus on lattices  $L$  that are critical points of  $\mathcal{F}_\mu$  in  $\mathcal{L}_d(V)$  for all  $V$  in an open interval. We show a result which is similar to the one obtained in [8, Sect. III] for energies of type  $E_f$  defined by (1.5), using tools from [20, 23].

We first recall the notion of strongly eutactic layer exactly as we have done it in [8, Sect. III].

**Definition 1.1 (Strongly eutactic layer).** Let  $L \in \mathcal{L}_d(1)$ . We say that a layer  $\mathfrak{m} = \{p \in L; |p| = \lambda\}$ , for some  $\lambda > 0$ , of  $L$  is strongly eutactic if  $\sharp \mathfrak{m} = 2k$  for some  $k \in \mathbb{N}$  and, for any  $x \in \mathbb{R}^d$ ,

$$\sum_{p \in \mathfrak{m}} \frac{(p \cdot x)^2}{|p|^2} = \frac{2k}{d} |x|^2.$$

**Remark 1.3.** After a suitable renormalization,  $\mathfrak{m}$  is also called a spherical 2-design (see [4]).

**Theorem 1.4 (Volume-stationary lattices for  $\mathcal{F}_\mu^\alpha$ ).** We assume that  $\Sigma$  is compact and  $\mu$  is radially symmetric. Then,  $L$  is a critical point of  $L \mapsto \mathcal{F}_{\mu_\lambda}(\lambda L)$  in  $\mathcal{L}_d(1)$  for all  $\lambda$  in an open interval  $I$  if and only if all the layers of  $L$  are strongly eutactic and  $I = (0, \infty)$ . In particular,  $L \in \{A_2, \mathbb{Z}^2, \mathbb{Z}^3, D_3, D_3^*\}$  in dimension  $d \in \{2, 3\}$ .

Therefore, considering only volume-stationary lattices allow to only compare the triangular and square lattices (resp. BCC, FCC and simple cubic lattices) in dimension 2 (resp. dimension 3). Furthermore, Theorem 1.4 tells us that  $A_2, \mathbb{Z}^2, \mathbb{Z}^3, D_3$  and  $D_3^*$  are critical points of  $\mathcal{F}_\mu^\alpha$  for any  $\alpha > 0$  and  $\mu$  radially symmetric on a ball  $\Sigma = B_R$  for any  $R > 0$ . In this case, combined with our numerical findings stated above (see also Section 5), we obtain new evidences that  $A_2$  and  $D_3$  are optimal for the grid cells problem if we restrict our study to volume-stationary lattices and radially symmetric firing field and measure  $\mu$ .

## 1.5 Conclusion and open problems

We conclude that, whereas the rigorous study of  $\mathcal{F}_\mu^\alpha$  stays a very challenging problem, our asymptotic and numerical investigations show new evidences of the optimality of the triangular and face-centred-cubic lattices for the grid cells problem. In particular, our results suggest the following conjecture:

**Conjecture 1.5 (Maximality of the best packing in dimensions 2 and 3).** *Let  $\sigma_R$  be the uniform measure on  $B_R$  and  $\alpha = \frac{10}{\pi}$ . Furthermore, let  $R_2 := \frac{1}{2}\sqrt{\frac{2}{\sqrt{3}}}$  and  $R_3 := 2^{-\frac{5}{6}}$ . Then we have:*

1. *For all  $R \leq R_2$ ,  $A_2$  is the unique maximizer of  $\mathcal{F}_{\sigma_R}^\alpha$  on  $\mathcal{L}_2(1)$ .*
2. *For all  $R \leq R_3$ ,  $D_3$  is the unique maximizer of  $\mathcal{F}_{\sigma_R}^\alpha$  on  $\mathcal{L}_3(1)$ .*

This problem by itself turns out to be a very interesting mathematical question with the need to derive new results for translated lattice theta functions. For instance, one may want to push further the properties of the Heat Kernel and to use the connection with  $\mathcal{F}_\mu^\alpha$  explained in Remark 2.1. It would also be interesting to study the  $\mu$ -dependence of the maximizer of  $\mathcal{F}_\mu^\alpha$ , in particular when  $\mu$  is not uniform nor radially symmetric. In the latter case, one could try to explain the existence of sheared grids observed for instance in [43], also for grid cells. Another direction of research would also be to replace the Gaussian function by another tuning curve and to study the same type of optimality problem. Finally, we think that our results and observation might be useful for other biological or physical models where periodic Fisher Information with Poisson statistics are involved.

**Plan of the paper.** In Section 2, we explain how we obtain formula (1.3) and on which biological assumptions we have built our model. Furthermore, the scaling formula (1.4) is shown in Proposition 2.2. Section 3 is devoted to the proof of Theorem 1.2 and to the alternative formula 3.1. The characterization of volume-stationary lattices is done in Section 4 where the proof of Theorem 1.4 is given. Finally, our numerical investigations are presented in Section 5 where we first discuss the parametrization of lattices as well as the properties of  $\mathcal{Q}_L^\alpha(y)$ .

## 2 Description of the model, derivation of formula (1.3) and scaling

In this section, we are justifying formula (1.3) by listing all our technical and biologically relevant assumptions. As explained in the introduction, we are following Mathis et al. [31] for building our model, with only small modifications.

We consider neurons (called grid cells) that are firing (spiking) according to the position (the stimulus)  $x \in \mathbb{R}^d$  of an animal. We are considering an arbitrary fixed time interval  $[0, T]$  where the neurons are spiking. We are assuming the following hypothesis **(A1)-(A6)** where the Gaussian is replaced by an arbitrary function  $f$  as in (1.5).

**(A1) Independence of neurons.** The neurons we consider are independently firing.

Given  $n$  independent neurons such that the  $i^{th}$  neuron fired  $k_i$  times in the time interval  $[0, T]$ , the probability of having  $K = (k_1, \dots, k_n)$  spikes when an animal is at position  $x \in \mathbb{R}^d$  is

$$P(K|x) = \prod_{i=1}^n P_i(k_i|x), \quad (2.1)$$

where  $P_i(k_i|x)$  is the probability of firing the  $i^{th}$  neuron  $k_i$  times when the animal is at  $x$ .

**(A2) Firing Poisson statistics.** The neuron's firing obey Poisson Statistics. More precisely, we assume that

$$P_i(k_i|x) = \frac{(\Omega_i(x))^{k_i} e^{-\Omega_i(x)}}{k_i!}, \quad (2.2)$$

where  $\Omega_i(x)$  is the average firing number of the  $i^{th}$  neuron at position  $x$  in the time interval  $[0, T]$ , also called its tuning curve.

**(A3) Long-range lattice-periodic tuning curve shape.** All the neuron's tuning curves are identically equal to

$$\Omega_i(x) = \Omega_L(x) = E_f[L + x] := \sum_{p \in L} f(|p + x|^2), \quad \forall i \in \{1, \dots, n\}, \quad (2.3)$$

for a lattice  $L \in \mathcal{L}_d(1)$  and a function  $f : [0, \infty) \rightarrow \mathbb{R}$  as in (1.5), in order for  $\Omega_L(x)$  to be absolutely convergent. We will call  $\Omega_L : \mathbb{R}^d \rightarrow \mathbb{R}_+$  the grid cell's tuning curve. When  $f$  has its maximum at  $r = 0$ , it means that there is more spikes when the animal cross a lattice site, which is the usual assumptions made on  $f$ . This tuning curve shape is slightly different than the periodic boundary conditions assumed by Mathis et al. in [31].

We define a grid module as an ensemble of  $N \in \mathbb{N}$  shifted grid cells  $\{\Omega_{L+y_j}\}_{j=1}^N$  where the vectors  $Y = (y_j)_j \subset \mathbb{R}^d$  are called the spatial phases of the module. Furthermore, we have for all  $x \in \mathbb{R}^d$ , all lattice  $L \in \mathcal{L}_d(1)$  and all shifting vector  $y_j \in Y$ ,

$$\Omega_{L+y_j}(x) = E_f[L + y_j + x] := \sum_{p \in L} f(|p + x + y_j|^2). \quad (2.4)$$

Therefore, for any spatial phase shifted by a vector  $y_j$ , we will write the probability in (2.1) as

$$P_j(K|x) = e^{-n\Omega_{L+y_j}(x)} \prod_{i=1}^n \frac{(\Omega_{L+y_j}(x))^{k_i}}{k_i!}, \quad j \in \{1, \dots, N\}. \quad (2.5)$$

As explained in [31], we are interested in solving the following mathematical question: given a spike count vector  $K = (k_1, \dots, k_n)$ , where is the animal? The estimation of this position is written  $\hat{x}(K)$ . We therefore want to minimize the square of the error in the decoding process which is given by

$$\varepsilon(x|\hat{x}) := \mathbb{E}_{P(K|x)} (\|x - \hat{x}(K)\|^2). \quad (2.6)$$

Minimizing the error  $\varepsilon(x|\hat{x})$  is the same as minimizing the trace of the covariance matrix  $\text{Cov}(x, \hat{x})$ . Furthermore, the Fisher Information (see e.g. [28]) is defined by the matrix  $J(x) = (J_{\ell,m}(x))_{\ell,m}$  where

$$J_{\ell,m}(x) = \int [\partial_{x_\ell} \log P(K|x) \partial_{x_m} \log P(K|x)] P(K|x) dK. \quad (2.7)$$

**(A4) Unbiased estimator assumption.** We assume that the Cramer-Rao lower bound holds (see e.g. [28]), i.e.  $\text{Cov}(x, \hat{x}) \geq J(x)^{-1}$ . This is automatically satisfied in the independent Poisson process case.

For the grid module, (A1) ensures that the Fisher Information is the sum of Fisher Informations for all the  $N$  spatially shifted phases  $Y$ , i.e.

$$J_{\ell,m}(x) = \sum_{j=1}^N \int [\partial_{x_\ell} \log P_j(K|x) \partial_{x_m} \log P_j(K|x)] P_j(K|x) dK. \quad (2.8)$$



A straightforward computation gives

$$\text{Tr}J(x) = \sum_{\ell=1}^d \sum_{j=1}^N (\partial_{x_\ell} \Omega_{L+y_j}(x))^2 \int \left( -n + \frac{\sum_{i=1}^n k_i}{\Omega_{L+y_j}(x)} \right)^2 P_j(K|x) dK. \quad (2.9)$$

The integral is in fact the Fisher Information of  $n$  independent Poisson processes with the same parameter  $\lambda = \Omega_{L+y_j}(x)$ , which means that it is  $n$  times the Fisher Information of one single Poisson process with the same parameter (see e.g. [28]). Therefore, for all  $y_j \in Y$ ,

$$\int \left( -n + \frac{\sum_{i=1}^n k_i}{\Omega_{L+y_j}(x)} \right)^2 P_j(K|x) dK = \frac{n}{\Omega_{L+y_j}(x)}. \quad (2.10)$$

We therefore obtain that

$$\text{Tr}J(x) = n \sum_{j=1}^N \mathcal{Q}_L(y_j + x), \quad \text{where} \quad \mathcal{Q}_L(y) := \frac{|\nabla_x E_f[L+y]|^2}{E_f[L+y]}. \quad (2.11)$$

Optimizing such lattice energy is a huge challenge since the maximizer varies a lot with  $x$  and  $Y$  (see Section 5). That is why it is not appropriate to our study. Therefore, we are again following [31] in order to transform the discrete set of shifts  $Y$  into a continuous set  $\Sigma$ .

**(A5) Aggregation of spatial phases.** We assume that  $\frac{1}{N} \sum_{j=1}^N \delta_{y_j} \rightarrow \mu \in \mathcal{M}(\Sigma)$  as  $N \rightarrow \infty$ , with

support in a compact set  $\Sigma \subset \mathbb{R}^2$ , which is observed in experiments (see [24]). The set  $\Sigma$  can be considered as the support of the grid cells module, also called the firing field of the module. Actually, there is a scale dependence between  $\Sigma$  and  $L$  in the sense that, if the distances in the lattice are multiplied by a real number  $\lambda$ , then it is the same for  $\Sigma$  (see e.g. [33, 42] and Proposition 2.2). Furthermore, it has been observed in [16] that the smallest width of  $\Sigma$  is 30cm-50cm for a side length (for the corresponding triangular lattice) of 50cm-1m, i.e. the different firing fields are not overlapping (as in Fig. 2). We also notice that, presented as above,  $\mu$  should be a probability measure. However, in the following we are considering a more general Radon measure.

Therefore, we want to maximize the following Fisher Information per neuron for the module  $M = (L, \Omega_L^\alpha, \mu, \Sigma)$ , where the limit is justified by the fact that  $y \mapsto \mathcal{Q}_L(y)$  is continuous and bounded on the compact set  $\Sigma$ ,

$$J_M(x) := \frac{1}{n} \lim_{N \rightarrow \infty} \frac{\text{Tr}J(x)}{N} = \int_{\Sigma} \frac{|\nabla_x \Omega_{L+y}(x)|^2}{\Omega_{L+y}(x)} d\mu(y) = \int_{\Sigma} \frac{|\nabla_x E_f[L+y+x]|^2}{E_f[L+y+x]} d\mu(y). \quad (2.12)$$

**(A6) Re-centering of the problem.** We assume that  $x = 0$ . Thus, the problem is simplified to maximize the resolution at  $x = 0$  of the decoding process.

Therefore, given  $f$  satisfying assumptions (1.5) and  $\mu \in \mathcal{M}(\Sigma)$ , we want to maximize among lattices  $L$  the following functional:

$$\mathcal{F}_\mu(L) = J_M(0) = \int_{\Sigma} \frac{|\nabla_y E_f[L+y]|^2}{E_f[L+y]} d\mu(y). \quad (2.13)$$

Furthermore, if  $f \geq 0$ , then we have the following more compact form

$$\mathcal{F}_\mu(L) = \int_{\Sigma} \left| \nabla_y \sqrt{E_f[L+y]} \right|^2 d\mu(y) \quad (2.14)$$

which gives us (1.3) by choosing  $f(r) = e^{-\pi\alpha r}$  and renaming the functional  $\mathcal{F}_\mu^\alpha$  to show the  $\alpha$ -dependence.

**Remark 2.1** (Fisher Information in terms of the Heat Kernel). It has to be noticed that  $\mathcal{F}_\mu^\alpha$  can be expressed in terms of the heat kernel on  $L$ . More precisely, and as we already pointed out in [11], let  $u_L(y, t)$  be the temperature at point  $y$  and at time  $t$ , if at initial time  $t = 0$  a heat source of unit strength is placed at each point of  $L$ , i.e.  $u_L$  is defined, for any lattice  $L \subset \mathbb{R}^d$ , any  $y \in \mathbb{R}^d$  and any  $t > 0$  as the solution of

$$\begin{cases} \partial_t u_L(y, t) = \Delta_y u_L & \text{for } (y, t) \in \mathbb{R}^d \times (0, \infty) \\ u_L(y, 0) = \sum_{p \in L} \delta_p & \text{for } y \in \mathbb{R}^d, \end{cases}$$

where  $\delta_p$  is the Dirac measure at  $p \in \mathbb{R}^d$ . Then, for any  $\alpha > 0$ , any lattice  $L \subset \mathbb{R}^d$  and any measure  $\mu \in \mathcal{M}(\Sigma)$ ,

$$\mathcal{F}_\mu^\alpha(L) = \frac{1}{\alpha^{\frac{d}{2}}} \int_\Sigma \left| \nabla_y \sqrt{u_L\left(y, \frac{1}{4\pi\alpha}\right)} \right|^2 d\mu(y). \quad (2.15)$$

We now show the scaling formula already known by Mathis et al. in [31, Eq (22)] and applied to the Gaussian periodic tuning curve. It is crucial to remember that, as recalled above and according to [33, 42], changing the density of the lattice  $L$  changes the size of the firing field  $\Sigma$  accordingly.

**Proposition 2.2 (Scaling formula).** *For any  $\lambda > 0$ , any  $\mu \in \mathcal{M}(\Sigma)$ , any  $L \in \mathcal{L}_d(1)$  and any  $\alpha > 0$ , we have*

$$\mathcal{F}_{\mu_\lambda}^\alpha(\lambda L) = \lambda^{-2} \mathcal{F}_\mu^{\lambda^2 \alpha}(L). \quad (2.16)$$

*Proof.* By a simple change of variable, we have

$$\begin{aligned} \mathcal{F}_{\mu_\lambda}^\alpha(\lambda L) &= \int_{\lambda \Sigma} \left| \nabla_y \sqrt{\theta_{\lambda L+y}(\alpha)} \right|^2 d\mu_\lambda(y) \\ &= \frac{1}{\lambda^2} \int_\Sigma \left| \nabla_y \sqrt{\theta_{\lambda L+\lambda y}(\alpha)} \right|^2 d\mu(y) \\ &= \frac{1}{\lambda^2} \int_\Sigma \left| \nabla_y \sqrt{\theta_{L+y}(\lambda^2 \alpha)} \right|^2 d\mu(y) = \lambda^{-2} \mathcal{F}_\mu^{\lambda^2 \alpha}(L). \end{aligned}$$

□

Since for any  $\alpha > 0$ , any  $\mu \in \mathcal{M}(\Sigma)$  and any  $L \in \mathcal{L}_d(1)$ ,  $\lim_{\lambda \rightarrow 0} \mathcal{F}_{\mu_\lambda}^\alpha(\lambda L) = \lim_{\lambda \rightarrow 0} \lambda^{-2} \mathcal{F}_\mu^{\lambda^2 \alpha}(L) = +\infty$ , it is sufficient to look for the maximizer of  $\mathcal{F}_\mu^\alpha$  for fixed  $\alpha$ ,  $\mu \in \mathcal{M}(\Sigma)$  and  $L \in \mathcal{L}_d(1)$ . If the density is not fixed, then it is then sufficient to take the high density limit to find  $+\infty$  as the maximum of  $\mathcal{F}_\mu^\alpha$ . Notice that we also have, for any  $\alpha > 0$ , any  $\mu \in \mathcal{M}(\Sigma)$  and  $L \in \mathcal{L}_d(1)$ ,  $\lim_{\lambda \rightarrow \infty} \mathcal{F}_{\mu_\lambda}^\alpha(\lambda L) = \lim_{\lambda \rightarrow \infty} \lambda^{-2} \mathcal{F}_\mu^{\lambda^2 \alpha}(L) = 0$ .

### 3 Alternative formula and proof of Theorem 1.2

We are proving Theorem 1.2 in this part, using an alternative formula given in [35].

**Proposition 3.1 (Alternative formula for  $\mathcal{F}_\mu^\alpha$ ).** *For any  $\alpha > 0$ , any  $\mu \in \mathcal{M}(\Sigma)$  and any  $L \in \mathcal{L}_d(1)$ ,*

$$\mathcal{F}_\mu^\alpha(L) = 4\pi^2 \alpha^2 \int_\Sigma \theta_{L+y}(\alpha) \left| \mathbb{E}[w]_{w \sim D_{L+y, \alpha}} \right|^2 d\mu(y), \quad (3.1)$$

where  $D_{L+x, \alpha}$  is the discrete Gaussian distribution over  $L+x$  with parameter  $\alpha$ , i.e. the probability distribution over  $L+x$  that assigns probability proportional to  $e^{-\pi\alpha|w|^2}$  to each vector  $w \in L+x$ .

*Proof.* Following [35, p. 6] (with  $s = \alpha^{-1/2}$ ), a straightforward computation gives

$$\frac{\nabla_x \theta_{L+x}(\alpha)}{\theta_{L+x}(\alpha)} = -2\pi\alpha \mathbb{E}_{w \sim D_{L+x, \alpha}}[w]. \quad (3.2)$$

It follows that

$$\frac{\|\nabla_y \theta_{L+y}(\alpha)\|^2}{\theta_{L+y}(\alpha)} = 4\pi^2 \alpha^2 \theta_{L+y}(\alpha) \left| \mathbb{E}_{w \sim D_{L+y, \alpha}}[w] \right|^2, \quad (3.3)$$

which shows (3.1).  $\square$

We now show Theorem 1.2 by directly applying (3.1).

*Proof of Theorem 1.2.* A straightforward computation shows that, for any  $\mu \in \mathcal{M}(\Sigma)$  and any  $\lambda > 0$ , as  $\alpha \rightarrow 0$ ,

$$\mathcal{F}_{\mu_\lambda}^\alpha(L) = 4\pi^2 \alpha^2 \int_\Sigma \theta_{L+y}(\alpha) \left| \mathbb{E}_{w \sim D_{L+y, \alpha}}[w] \right|^2 d\mu_\lambda(y) \sim 4\pi^2 \alpha^2 \int_\Sigma \theta_{L+y}(\alpha) d\mu_\lambda(y), \quad (3.4)$$

which is uniquely minimized by  $A_2$  (resp. locally minimized by  $D_3^*$ ) by a direct application of [12, Thm. 2 and 3] (resp. [9, Thm. 4.3]) as  $\lambda$  is small enough or if  $\mu$  has the form  $d\mu(x) = \rho(|x|^2)dx$  and  $\rho$  is a completely monotone function. The fact that  $\mathcal{F}_{\mu_\lambda}^\alpha$  does not have any maximizer as  $\alpha, \lambda$  are small enough is again a simple consequence of our work in [9] and the fact that the lattice theta function  $L \mapsto \theta_L(\alpha)$  does not have a maximizer in  $\mathcal{L}_d(1)$ . Indeed, it is enough to take a sequence of orthorhombic lattices with degenerate shapes for showing that the theta functions goes to infinity.  $\square$

**Remark 3.2.** The same is true in dimensions  $d \in \{8, 24\}$  replacing  $A_2$  by  $E_8$  or  $A_{24}$ , again by an application of [9, Thm 4.5] and the universal optimality of these lattices shown in [18].

## 4 Volume-stationary lattices - Proof of Theorem 1.4

We now show Theorem 1.4 by using a combination of Proposition 2.2, formula (3.1) and our works in [12] and [8].

*Proof of Theorem 1.4.* We consider  $\mathcal{F}_{\mu_\lambda}^\alpha(\lambda L)$  for  $\lambda > 0$ , then by assumption we have that  $\nabla_L \mathcal{F}_{\mu_\lambda}^\alpha(\lambda L) = 0$  for all  $\lambda \in I$ , where  $I$  is an open interval of  $\mathbb{R}_+$ . We therefore have, for all  $\lambda \in I$ ,

$$\nabla_L \int_\Sigma \left| \nabla_y \sqrt{\theta_{\lambda L+y}(\alpha)} \right|^2 d\mu(y) = 0. \quad (4.1)$$

Since  $\lambda \mapsto \nabla_L \mathcal{F}_{\mu_\lambda}^\alpha(\lambda L)$  is analytic, it follows that  $I = (0, \infty)$ . We now use formula (3.1) combined with Proposition 2.2 and we get

$$\mathcal{F}_{\mu_\lambda}^\alpha(\lambda L) = \lambda^{-2} \mathcal{F}_\mu^{\lambda^2 \alpha}(L) = 4\pi^2 \lambda^2 \alpha^2 \int_\Sigma \theta_{L+y}(\lambda^2 \alpha) \left| \mathbb{E}_{w \sim D_{L+y, \lambda^2 \alpha}}[w] \right|^2 d\mu(y).$$

Therefore, we obtain for  $\lambda < \lambda_0$  sufficiently small,

$$\nabla_L \left\{ \int_\Sigma \theta_{L+y}(\lambda^2 \alpha) d\mu(y) \right\} = 0. \quad (4.2)$$

As in [12], using Poisson summation formula and analyticity again, it follows that, for all  $\lambda > 0$ ,

$$\nabla_L \sum_{q \in L^*} e^{-\frac{\pi}{\alpha \lambda^2} |q|^2} \hat{\mu}(q) = 0. \quad (4.3)$$

Since  $\mu$  is radially symmetric, then its Fourier transform is radially symmetric, i.e.  $\hat{\mu}(q) = h(|q|)$  for some function  $h$ . Now, the same argument can be used as in [8, 20, 23] to conclude that the first layer of  $L^*$  must be strongly eutactic since (4.3) implies the same result for the lattice theta function  $\nabla_L \theta_{L^*}(1/(\alpha\lambda)) = 0$  for all  $\lambda < \lambda_0$ , and then for the Epstein zeta function  $\zeta_L(s)$  for all  $s > 0$  as a simple consequence. Therefore we deduce that all of the layers have to satisfy the same property. It follows that  $L^*$  is one of the lattices listed in the theorem's statement (see e.g. [23, Corollary 2]), which is equivalent with the fact that  $L$  belongs exactly to this list.  $\square$

**Remark 4.1.** The proof still holds if the Gaussian is replaced by a function  $f$  which is the Laplace transform of a measure. We also suspect that the result is also true for some non-radially symmetric measure  $\mu$ .

## 5 Numerical investigation

We are using the software Scilab to perform our numerics. All the values are computed by using a sufficient number of points for estimating our infinite sums according to the value of  $\alpha$  we choose (mostly  $\alpha = \frac{10}{\pi} \approx 3.18$ ) for which terms are going to zero very quickly as the distances increase.

### 5.1 Parametrization of lattices in dimension 2 and 3

We recall here how to parametrize a  $d$ -dimensional lattice in order to perform our numerical investigation. We basically follow the lines of [6, 7] by stating that a two-dimensional (resp. three-dimensional) lattice of unit density can be parametrized by two real numbers  $(x, y)$  (resp. five real numbers  $(u, v, x, y, z)$ ) belonging to a fundamental domain  $\mathcal{D}_2 \subset \mathbb{R}^2$  (resp.  $\mathcal{D}_3 \subset \mathbb{R}^5$ ) where only one copy of each lattice appears (see e.g. [44, Sect. 1.4]). More precisely, two-dimensional and three-dimensional lattices can be written respectively as

$$L = \mathbb{Z} \left( \frac{1}{\sqrt{y}}, 0 \right) \oplus \mathbb{Z} \left( \frac{x}{\sqrt{y}}, \sqrt{y} \right),$$

$$L = 2^{\frac{1}{6}} \left[ \mathbb{Z} \left( \frac{1}{\sqrt{u}}, 0, 0 \right) \oplus \mathbb{Z} \left( \frac{x}{\sqrt{u}}, \frac{v}{\sqrt{u}}, 0 \right) \oplus \mathbb{Z} \left( \frac{y}{\sqrt{u}}, \frac{vz}{\sqrt{u}}, \frac{u}{v\sqrt{2}} \right) \right].$$

In dimension  $d = 2$ , this domain is easy to describe whereas it is more complicated in dimension  $d = 3$ . In particular, we have

$$\mathcal{D}_2 := \left\{ (x, y) \in \mathbb{R}^2 : 0 \leq x \leq \frac{1}{2}, y > 0, x^2 + y^2 \geq 1 \right\}.$$

The square lattice  $\mathbb{Z}^2$  and triangular lattice  $A_2$  are respectively represented by  $(0, 1) \in \mathcal{D}_2$  and  $\left(\frac{1}{2}, \frac{\sqrt{3}}{2}\right) \in \mathcal{D}_2$ . We omit to write what an example of fundamental domain of  $\mathcal{L}_3(1)$  could be, but we recall that the simple cubic lattice  $\mathbb{Z}^3$ , the FCC lattice  $D_3$  and the BCC lattice  $D_3^*$  are respectively represented by  $(2^{1/3}, 1, 0, 0, 0) \in \mathcal{D}_3$ ,  $(1, 1, 0, 1/2, 1/2) \in \mathcal{D}_3$  and  $(2^{-1/3}, 1, 0, 1/2, 1/2) \in \mathcal{D}_3$ . We recall that, since the three-dimensional case is too demanding in terms of computational time, we will only compare certain lattices and compute the Hessian at the FCC lattice.

### 5.2 The pure discrete case: combinations of $\mathcal{Q}_L(y)$

We first explain why the problem of maximizing the discrete version of the Fisher Information's trace (2.11) (choosing again  $x = 0$ ), i.e.

$$\text{Tr} J(0) = n \sum_{j=1}^N \mathcal{Q}_L(y_j), \quad \mathcal{Q}_L(y) := \frac{|\nabla_y \theta_{L+y}(\alpha)|^2}{\theta_{L+y}(\alpha)},$$

is very difficult and therefore why – besides the above biological justification – it is convenient to consider a continuous firing field  $\Sigma$  instead of a set of points  $Y$ . We only consider the two-dimensional case, but the same remarks hold for higher dimensions.

For any  $L = \bigoplus_{i=1}^d \mathbb{Z}u_i$ , if for all  $j \in \{1, \dots, N\}$ ,  $y_j \in \{u_i, \frac{u_i}{2}, \frac{1}{2} \sum_i u_i\}$  for any  $i \in \{1, \dots, d\}$ , then  $\text{Tr}J(0) = 0$  since these points  $y_j$  are known to be critical points for  $y \mapsto \theta_{L+y}(\alpha)$  – and more generally  $y \mapsto E_f[L+Y]$  for any function  $f$  decaying sufficiently fast at infinity. In the particular case  $L = A_2$ , the barycenters of the primitive triangles are also critical points of  $y \mapsto \theta_{L+y}(\alpha)$  for all  $\alpha > 0$  as shown in [5] (see Fig. 4). Furthermore, in Fig. 3, we show that the maximizer of  $\text{Tr}J(0)$  varies a lot with  $\{y_j\}_j$ .

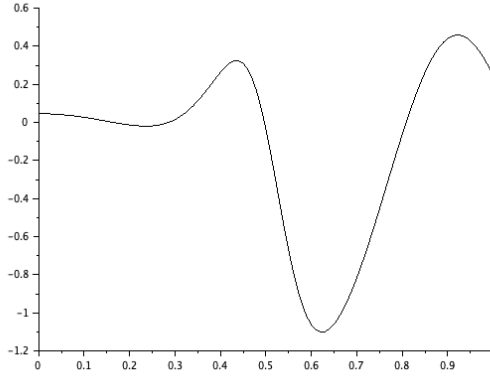


Figure 3: Plot of  $t \mapsto \mathcal{Q}_{A_2}^\alpha(0.1, 0.1) + \mathcal{Q}_{A_2}^\alpha(t, 0.2) - (\mathcal{Q}_{\mathbb{Z}^2}^\alpha(0.1, 0.1) + \mathcal{Q}_{\mathbb{Z}^2}^\alpha(t, 0.2))$  for  $\alpha = \frac{10}{\pi}$  and  $t \in [0, 1]$ , showing that the maximizer of  $\text{Tr}J_M(0)$  is not always triangular.

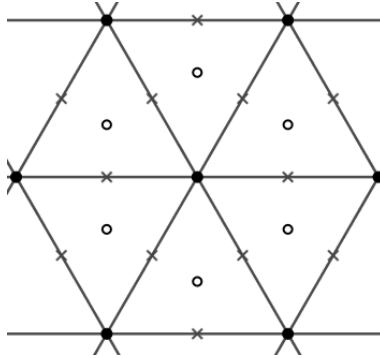


Figure 4: Zeros of  $x \mapsto \nabla_x \theta_{A_2+x}(\alpha)$  in a patch of  $A_2$ . Following [5],  $\bullet$  are the maximizers,  $\circ$  the minimizers and  $\times$  the saddle points of the function  $x \mapsto \theta_{A_2+x}(\alpha)$ . These are the only critical points of this function.

Furthermore  $L \mapsto \mathcal{Q}_L^\alpha(y)$  alone is not always maximized by the same lattice as  $y$  varies in  $\Sigma = B_R$ . Indeed, writing  $y = (r \cos \theta, r \sin \theta)$  and fixing  $r$ , we compare the energies of the square and triangular lattices by plotting

$$\theta \mapsto g_r(\theta) := \mathcal{Q}_{\mathbb{Z}^2}^\alpha(r \cos \theta, r \sin \theta) - \mathcal{Q}_{A_2}^\alpha(r \cos \theta, r \sin \theta), \quad \alpha = \frac{10}{\pi}. \quad (5.1)$$

Our observation are the following (see Fig. 5):

- For small  $r$ , we observe that  $g_r(\theta) < 0$  for all  $\theta \in [0, 2\pi]$ . The triangular lattice has higher energy than the square lattice.

- For  $r > 0.24$ , there are alternation of signs for  $g_r$  on some intervals of  $[0, 2\pi]$ .
- For  $r = 0.6$ , the positive part of  $g_r$  is more important than the negative one.

It follows that integrating on a ball with radius larger than  $R_0 = 0.24$  makes the proof of maximality of  $A_2$  much more difficult. Furthermore, it is not surprising that the triangular lattice is almost never a critical point of the integrand in  $\mathcal{L}_2(1)$  (see for instance Fig. 6).

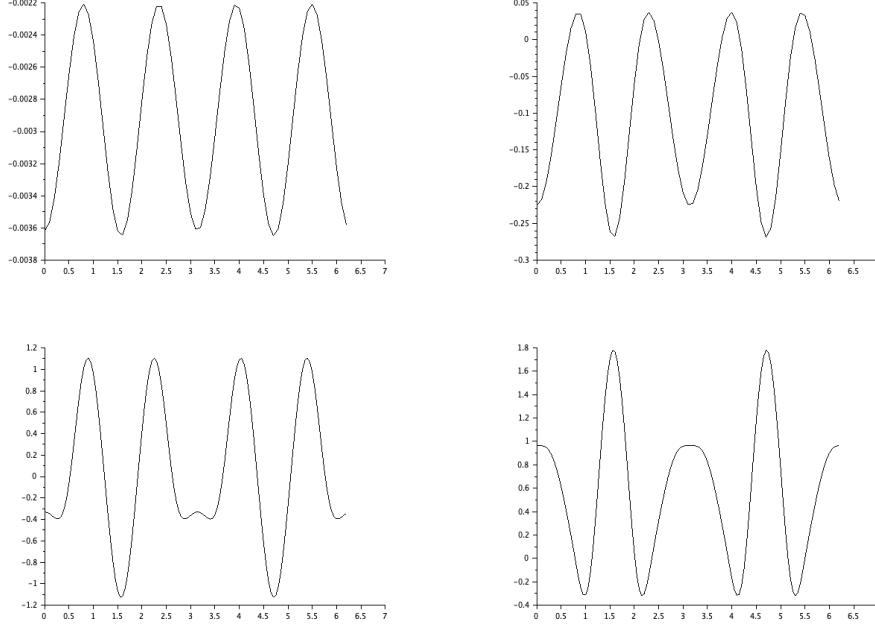


Figure 5: Plots of  $g_r$  (see (5.1)) on  $[0, 2\pi]$  for  $r \in \{0.1, 0.3, 0.5, 0.6\}$  in reading direction.

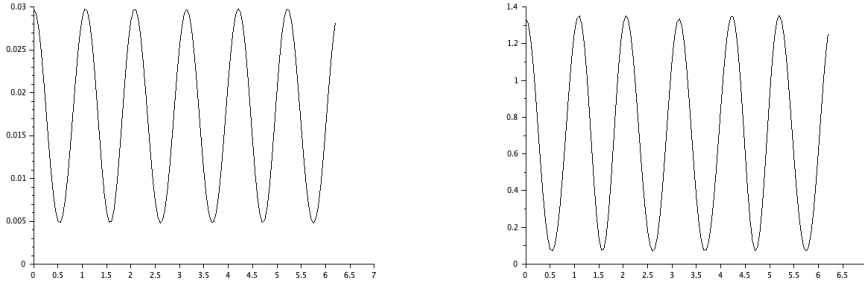


Figure 6: Plot of  $\theta \mapsto \|\nabla_L Q_L^\alpha(r \cos \theta, r \sin \theta)\|^2$  for  $\theta \in [0, 2\pi]$  and fixed  $r \in \{0.2, 0.3\}$ .

### 5.3 Dimension 2

We are considering the  $\alpha = \frac{10}{\pi}$  case (see Fig. 7), in such a way that

$$\theta_{L+y}(\alpha) = \sum_{p \in L} e^{-10|p+y|^2}.$$

We are also assuming that  $\mu = \sigma_R$  is the uniform measure on  $\Sigma = B_R$  for some  $R > 0$ . For simplicity, we omit to renormalize the measure, in such a way that  $\mu$  is almost never a probability

measure. It does not matter in our study since we are considering optimizers at fixed  $R$ .

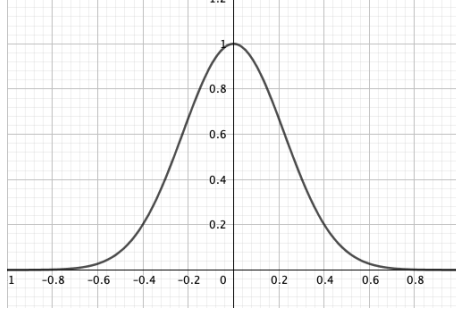


Figure 7: Plot of  $r \mapsto f(r^2) = e^{-10r^2}$ .

We observe that for  $R \in \{0.1, 0.2, 0.3, 0.4, 0.5\}$ , the triangular lattice  $A_2$  is the unique maximizer of  $\mathcal{F}_\mu^\alpha$  in  $\mathcal{L}_2(1)$ . In Fig. 8, we give one example of our numerical outputs as a contour plot for the particular case  $R = 0.5$ . We have also checked that the same maximality result holds for  $R = \frac{1}{2}\sqrt{\frac{2}{3}}$  being the half side length of  $A_2$ , i.e. the radius of the balls reaching the densest lattice packing of unit density in  $\mathbb{R}^2$ . If  $R > 0.6$ , the square lattice has a higher energy than the triangular one and the functional does not have any maximizer.

In order to illustrate Theorem 1.2, we choose  $\alpha = \frac{2}{\pi}$ ,  $\Sigma = B_R$ ,  $\mu = \sigma_R$ , and we observe in Fig. 9) that for  $R = 0.1$ ,  $A_2$  is the unique minimizer of  $\mathcal{F}_\mu^\alpha$  in  $\mathcal{L}_2(1)$  and the functional does not have any maximizer.

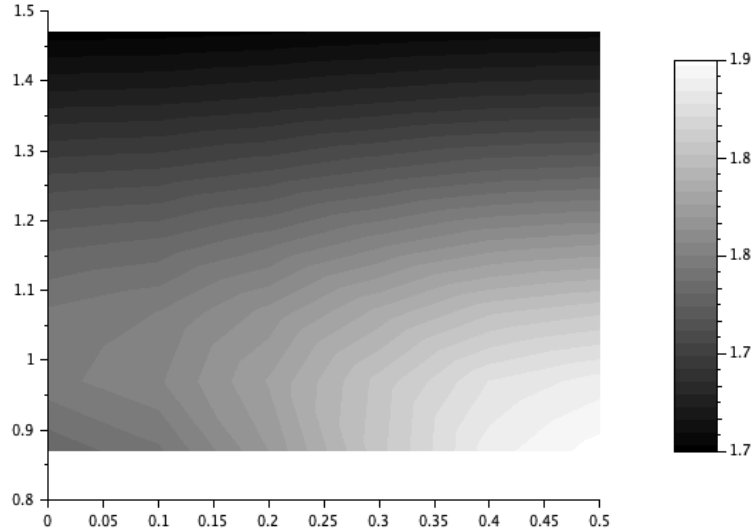


Figure 8: Case  $\mu = \sigma_R$  uniform on  $\Sigma = B_R$ ,  $R = 0.5$  and  $\alpha = \frac{10}{\pi}$ . The triangular lattice  $A_2$ , corresponding to the point  $(1/2, \sqrt{3}/2)$ , is the unique maximizer of  $\mathcal{F}_\mu^\alpha$  in  $\mathcal{L}_2(1)$ .

If we compare the Fisher Informations of the two-dimensional volume-stationary lattices, i.e.  $A_2$  and  $\mathbb{Z}^2$  for fixed  $\alpha = 10/\pi$  and increasing  $R$ , we obtain the graph of Fig. 10. We observe that, for  $R \in [0.1, 0.57]$ ,  $\mathcal{F}_{\sigma_R}^\alpha(A_2) > \mathcal{F}_{\sigma_R}^\alpha(\mathbb{Z}^2)$  whereas the square lattice has a higher Fisher Information for  $R \in [0.58, 0.7]$ . We also remark that the firing fields start to overlap when  $R > \frac{1}{2}\sqrt{\frac{2}{3}} \approx 0.5373$ .

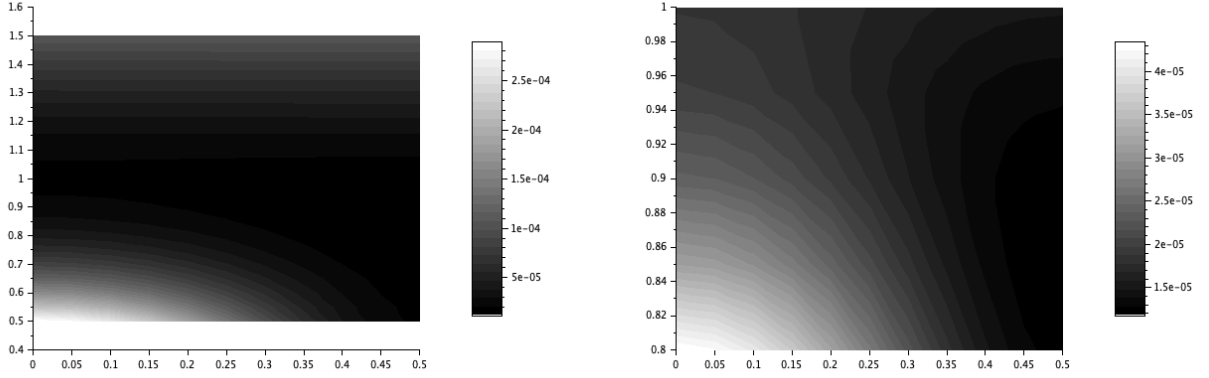


Figure 9: Illustration of Theorem 1.2. Case  $\mu = \sigma_R$  uniform on  $\Sigma = B_R$ ,  $R = 0.1$  and  $\alpha = \frac{2}{\pi}$ . There is no maximizer (left). Furthermore, the triangular lattice  $A_2$ , corresponding to the point  $(1/2, \sqrt{3}/2)$ , is the unique minimizer of  $\mathcal{F}_\mu^\alpha$  in  $\mathcal{L}_2(1)$ .

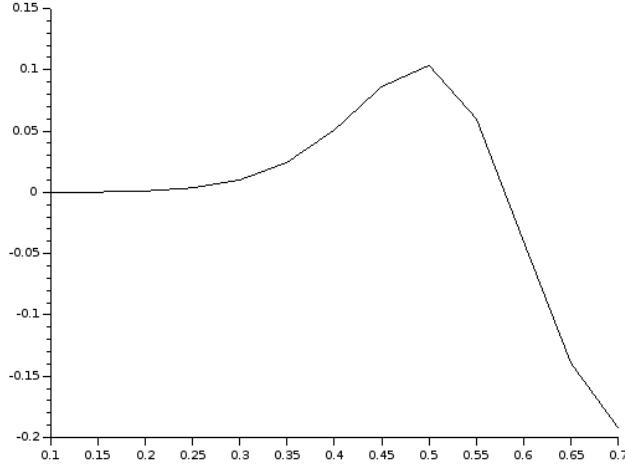


Figure 10: Plot of  $R \mapsto \mathcal{F}_{\sigma_R}^\alpha(A_2) - \mathcal{F}_{\sigma_R}^\alpha(\mathbb{Z}^2)$  where  $\alpha = \frac{10}{\pi}$  and  $\sigma_R$  is the uniform measure on  $\Sigma = B_R$ , for  $R \in [0.1, 0.7]$ .

## 5.4 Dimension 3

For our investigation in dimension  $d = 3$ , we have again chosen  $\alpha = \frac{10}{\pi}$ . Since the numerical computations are very demanding, we are only giving the following type of results: local optimality results and comparisons of volume-stationary lattices, i.e.  $\mathbb{Z}^3, D_3$  and  $D_3^*$ .

As in the previous section on two-dimensional lattices, it is clear that  $D_3, D_3^*$  and  $\mathbb{Z}^3$  are almost never critical points for  $L \mapsto \mathcal{Q}_L^\alpha(y)$  for a given  $y$ . It is only true for some points  $y$  being the hole or deep holes of  $L$  (center of cells, midpoints, etc.) as we have already explained for  $A_2$  (see Fig. 3). It is therefore not enough to only study  $L \mapsto \mathcal{Q}_L^\alpha(y)$  in order to investigate the extrema of  $\mathcal{F}_\mu^\alpha$ .

By comparing  $\mathcal{Q}_L^\alpha(y)$  for  $y \in \Sigma = B_R$ , we observe that there exists  $R_0 \approx 0.1$  such that

$$\mathcal{Q}_{D_3}(y) > \mathcal{Q}_{D_3^*}(y) > \mathcal{Q}_{\mathbb{Z}^3}(y), \quad \forall y \in B_{R_0},$$



which directly means that, for  $\mu = \sigma_{R_0}$ ,

$$\mathcal{F}_\mu^\alpha(\mathbf{D}_3) > \mathcal{F}_\mu^\alpha(\mathbf{D}_3^*) > \mathcal{F}_\mu^\alpha(\mathbb{Z}^3). \quad (5.2)$$

This result, which could thus follow from a direct analysis of  $\mathcal{Q}_L^\alpha$ , is not totally relevant biologically. Indeed, the radius of the firing field  $\Sigma = B_R$  should be close (actually slightly smaller) to  $R_{\mathbf{D}_3} = 2^{-5/6} \approx 0.56123$  which is the half side length of the FCC lattice, i.e. the radius of balls reaching the densest lattice packing of unit density in  $\mathbb{R}^3$ . Not surprisingly if we compare with the two-dimensional case, we have also checked on a set of discrete values of  $R$  that (5.2) still holds for  $R \in [0.1, 0.57]$ .

Furthermore, we have also numerically checked the local maximality of  $\mathbf{D}_3$  for radii  $R \in \{0.1, 0.2, 0.3, 0.4, 0.5, 2^{-5/6}\}$  by computing the Hessian of  $\mathcal{F}_\mu^\alpha$  at  $L = \mathbf{D}_3$  which appears to be definite positive in all these cases.

**Acknowledgement:** I would like to thank the Austrian Science Fund (FWF) for its financial support through the project F65.

## References

- [1] A. Abrikosov. The Magnetic Properties of Superconducting Alloys. *Journal of Physics and Chemistry of Solids*, 2:199–208, 1957.
- [2] F. Anselmi, M.M. Murray, and B. Franceschiello. A computational model for grid maps in neural populations. *Journal of Computational Neuroscience*, 48:149–159, 2020.
- [3] M. Antlanger, G. Kahl, M. Mazars, L. Samaj, and E. Trizac. Rich polymorphic behavior of Wigner bilayers. *Physical Review Letters*, 117(11):118002, 2016.
- [4] C. Bachoc and B. Venkov. Modular Forms, Lattices and Spherical Designs. *Réseaux euclidiens, designs sphériques et groupes*, L’Ens. Math.(Monographie 37, J. Martinet, ed.):87–111, 2001.
- [5] A. Baernstein II. A minimum problem for heat kernels of flat tori. *Contemp. Math.*, 201:227–243, 1997.
- [6] L. Bétermin. Local variational study of 2d lattice energies and application to Lennard-Jones type interactions. *Nonlinearity*, 31(9):3973–4005, 2018.
- [7] L. Bétermin. Local optimality of cubic lattices for interaction energies. *Anal. Math. Phys.*, 9(1):403–426, 2019.
- [8] L. Bétermin. Minimizing lattice structures for Morse potential energy in two and three dimensions. *J. Math. Phys.*, 60(10):102901, 2019.
- [9] L. Bétermin. Minimal Soft Lattice Theta Functions. *Constr. Approx.*, 52(1):115–138, 2020.
- [10] L. Bétermin and M. Faulhuber. Maximal theta functions - Universal optimality of the hexagonal lattice for Madelung-like lattice energies. *Preprint. arXiv:2007.15977*, 2020.
- [11] L. Bétermin and H. Knüpfer. On Born’s conjecture about optimal distribution of charges for an infinite ionic crystal. *J. Nonlinear Sci.*, 28(5):1629–1656, 2018.
- [12] L. Bétermin and H. Knüpfer. Optimal lattice configurations for interacting spatially extended particles. *Lett. Math. Phys.*, 108(10):2213–2228, 2018.
- [13] L. Bétermin and M. Petrache. Dimension reduction techniques for the minimization of theta functions on lattices. *J. Math. Phys.*, 58:071902, 2017.
- [14] L. Bétermin and M. Petrache. Optimal and non-optimal lattices for non-completely monotone interaction potentials. *Anal. Math. Phys.*, 9(4):2033–2073, 2019.
- [15] X. Blanc and M. Lewin. The Crystallization Conjecture: A Review. *EMS Surv. in Math. Sci.*, 2:255–306, 2015.
- [16] V.H. Brun, T. Solstad, K.B. Kjelstrup, M. Fyhn, M.P. Witter, E.I. Moser, and M.B. Moser. Progressive increase in grid scale from dorsal to ventral medial entorhinal cortex. *Hippocampus*, 18:1200–1212, 2008.
- [17] H. Cohn, A. Kumar, S. D. Miller, D. Radchenko, and M. Viazovska. The sphere packing problem in dimension 24. *Ann. of Math.*, 185(3):1017–1033, 2017.
- [18] H. Cohn, A. Kumar, S. D. Miller, D. Radchenko, and M. Viazovska. Universal optimality of the  $E_8$  and Leech lattices and interpolation formulas. *Preprint. arXiv:1902.05438*, 2019.
- [19] T. D’Albis and R. Kempfer. A single-cell spiking model for the origin of grid-cell patterns. *PLoS Comput Biol*, 13(10):e1005782, 2017.

- [20] B. N. Delone and S. S. Ryshkov. A Contribution to the Theory of the Extrema of a Multidimensional zeta-function. *Dokl. Akad. Nauk SSSR*, 173(4):991–994, 1967.
- [21] M. Faulhuber and S. Steinerberger. Optimal Gabor frame bounds for separable lattices and estimates for Jacobi theta functions. *J. Math. Anal. Appl.*, 445(1):407–422, 2017.
- [22] K. Gerlei, J. Passlack, I. Hawes, B. Vandrey, H. Stevens, I. Papastathopoulos, and M.F. Nolan. Grid cells are modulated by local head direction. *Nature Communications*, 11(4228), 2020.
- [23] P. M. Gruber. Application of an Idea of Voronoi to Lattice Zeta Functions. *Proc. Steklov Inst. Math.*, 276:103–124, 2012.
- [24] T. Hafting, M. Fyhn, S. Molden, M.B. Moser, and E.I. Moser. Microstructure of a spatial map in the entorhinal cortex. *Nature*, 436:801–6, 2005.
- [25] R. C. Heitmann and C. Radin. The Ground State for Sticky Disks. *J. Stat. Phys.*, 22:281–287, 1980.
- [26] L. Kantorovich. *Quantum Theory of the Solid State*. Fundamental Theories of Physics. Springer Netherlands, 1st edition edition, 2004.
- [27] M. Kim and E.A. Maguire. Can we study 3D grid codes non-invasively in the human brain? Methodological considerations and fMRI findings. *Neuroimage*, 186:667–678, 2019.
- [28] E.L. Lehmann. *Theory of Point estimation*. NY, USA: Springer-Verlag, 2nd edition edition, 1998.
- [29] S. Luo, X. Ren, and J. Wei. Non-hexagonal lattices from a two species interacting system. *SIAM J. Math. Anal.*, 52(2):1903–1942, 2020. *Preprint. arXiv:1902.09611*.
- [30] S. Luo and J. Wei. On minima of sum of theta functions and Mueller-Ho Conjecture. *Preprint. arXiv:2004.13882*, 2020.
- [31] A. Mathis, M.B. Stemmier, and A.V.M. Herz. Probable nature of higher-dimensional symmetries underlying mammalian grid-cell activity patterns. *eLife* 2015.4, pages 1–29, 2015.
- [32] H. L. Montgomery. Minimal Theta Functions. *Glasg. Math. J.*, 30(1):75–85, 1988.
- [33] G.J. Quirk, R.U. Muller, J.L. Kubie, and J.B. Ranck Jr. The positional firing properties of medial entorhinal neurons: Description and comparison with hippocampal place cells. *J Neurosci*, 12:1945–1963, 1992.
- [34] C. Radin. Low temperature and the origin of crystalline symmetry. *International Journal of Modern Physics B*, 1(5 and 6):1157–1191, 1987.
- [35] O. Regev and N. Stephens-Davidowitz. An Inequality for Gaussians on Lattices. *Preprint. arXiv:1502.04796*, 02 2015.
- [36] S. Rosay, S. Weber, and M. Mulas. Modeling grid fields instead of modeling grid cells. *Journal of Computational Neuroscience*, 47:43–60, 2019.
- [37] D.C. Rowland, Y. Roudi, M.B. Moser, and E.I. Moser. Ten years of grid cells. *Annual Review of Neuroscience*, 39(19-40), 2016.
- [38] E. Sandier and S. Serfaty. From the Ginzburg-Landau Model to Vortex Lattice Problems. *Comm. Math. Phys.*, 313(3):635–743, 2012.
- [39] P. Sarnak and A. Strömbergsson. Minima of Epstein’s Zeta Function and Heights of Flat Tori. *Invent. Math.*, 165:115–151, 2006.
- [40] T. Solstad, E.I. Moser, and G.T. Einevoll. From grid cells to place cells: A mathematical model. *Hippocampus*, 16:1026–1031, 2006.
- [41] B. Sorscher, G.C. Mel, S. Ganguli, and S.A. Ocko. A unified theory for the origin of grid cells through the lens of pattern formation. In *Advances in Neural Information Processing Systems 32*, pages 10003–10013. Curran Associates, Inc., 2019.
- [42] H. Stensola, T. Stensola, T. Solstad, K. Frøland, M.B. Moser, and E.I. Moser. The entorhinal grid map is discretized. *Nature*, 492:72–78, 2012.
- [43] T. Stensola, H. Stensola, M.B. Moser, and E.I. Moser. Shearing-induced asymmetry in entorhinal grid cells. *Nature*, 518:207–212, 2015.
- [44] A. Terras. *Harmonic Analysis on Symmetric Spaces and Applications II*. Springer New York, 1988.
- [45] B.W. Towse, C. Barry, D. Bush, and N. Burgess. Optimal configurations of spatial scale for grid cell firing under noise and uncertainty. *Phil. Trans. R. Soc. B*, 369:20130290, 2014.
- [46] M. Viazovska. The sphere packing problem in dimension 8. *Ann. of Math.*, 185(3):991–1015, 2017.
- [47] X.-X Wei, J. Prentice, and V. Balasubramanian. A principle of economy predicts the functional architecture of grid cells. *Elife*, 4(e08362), 2015.
- [48] M.M. Yartsev and N. Ulanovsky. Representation of Three-Dimensional Space in the Hippocampus of Flying Bats. *Science*, 340(6130):367–372, 2013.